Journal of Civil Engineering and Urban Planning (2022)
Clausius Scientific Press, Canada

DOI: 10.23977/jceup.2022.040304
ISSN 2616-3969 Vol. 4 Num. 3

Analysis of Landslide Damage Mechanisms and Control Options for Binary Structures under Heavy Rainfall Conditions

Xu Feng*, Shuangyang Cai, Ming Zhou

Hunan Institute of Traffic Engineering, Hengyang, China
**Corresponding author*

Keywords: Slope engineering, heavy rainfall, binary structures, landslide damage mechanism, finite element simulation

Abstract: According to statistics, more than 90% of landslide accidents are closely related to the action of water. To determine the damage mechanism of binary structure landslide under rainfall conditions, the numerical model of binary structure slope under strong rainfall conditions is established by the finite element software Midas-GTS, relying on the slope project of an industrial park in Hunan. By studying the changes in stability safety factor, stress field, and seepage field of the slope in the process of heavy rainfall, the damage mechanism of the binary structure slope under the condition of heavy rainfall is analyzed and deduced. The results show that the damage of binary structure landslide can be divided into four evolutionary processes: (1) Nurturing stage: After excavation and slope cutting, the strongly weathered layer and part of the medium weathered layer of mudstone are exposed to the air, and the rocks will be deformed after long-term weathering and water immersion, resulting in the reduction of their strength; (2) Cracking stage: As time passes, surface water continues to penetrate downward along the fissures and soil traps, resulting in the formation of multiple penetrating fissures inside the soil body. formation of multiple penetrating fissures; (3) Creep phase: Frequent heavy rainfall causes the geotechnical body to gradually saturate, the overlying load continues to increase, the driving force of the landslide also continues to increase, the mudstone further softens, the geotechnical body shear strength decreases, and the slip zone gradually develops downward; (4) Sliding phase: Long-term precipitation causes the geotechnical body near the slip surface shear strength decreases, insufficient to support the upper load, the slip surface gradually develops through (4) Sliding stage: Long-term precipitation causes the shear strength of the geotechnical body near the slip surface to decrease, which is insufficient to support the upper load, and the slip surface gradually develops through.

1. Introduction

In Hunan, the rainy season is abundant, and geological hazards such as landslides, landslides, and debris flows are frequent. Among them, landslides, as one of the most widely distributed geological hazards, have been focused on the analysis of landslide damage mechanisms by a wide range of

scholars due to their many influencing factors and complex geological conditions [1-7]. Sun Feng et al. used a non-linear analysis of an elastic-plastic dynamic consolidation large deformation finite element model to verify the deformation and damage mechanism of a debris soil landslide [8]; Ai Weng et al. used the Yushu seismic wave as the basic dynamic load for the test [9], and used the Yushu Airport Road pile-up landslide as the test prototype to verify the progressive damage mechanism and characteristics of a multi-sliding surface landslide through large shaking table experiments; Zhou Qingfeng et al. investigated the fractured The study showed that the strong tectonic action led to abnormal development of rock joints and fractures [10, 11], and the integrity of the rock body was damaged. The analysis was carried out to determine the damage to the landslide zone under the action of fracture water pressure at the trailing edge of different water-filling heights.

The above-mentioned studies have carried out various analyses of slope damage modes for various causes, but no systematic analysis of the damage mechanism of binary structure landslides induced by heavy precipitation has been seen. Because of this, taking a landslide accident in an industrial park in Hunan Province as an example and combining the site investigation data, a damage theory study was conducted on the slope instability process to the damage mode of binary structure pushed landslide under heavy rainfall conditions.

2. Overview of the Project and Basic Geological Conditions of the Slope

2.1. Overview of the Project

In April 2018, a Hunan industrial park proposed to excavate a new municipal road next to a chemical plant. The road section was excavated to form two road graben slopes in the north and south, the slope body in the north is relatively low and the deformation is relatively small; The south side is the uphill side, the slope is 14m high, and is a secondary slope, the primary slope is 8m high, the platform is 2m wide and the second slope is 6m high the south slope body is the main object of this study. The slope and the surrounding buildings have been constructed for a long time and the slope has not been reinforced in recent years. According to the site investigation in the survey area, the front edge of the slope is free of obvious uplift, but the trailing edge has obvious cracking and is in an unstable state. Several cracks, generally 5-8 m long and 5-10 cm wide, were found on the trailing edge of the slope slides occurred after suffering continuous heavy rainfall during the rainy weather in May 2018. This is shown in Figure 1.

Figure 1: Engineering landslide site.

2.2. Basic Geological Conditions

2.2.1. Climatic Conditions

The region has a subtropical continental climate with abundant heat, rainfall, distinct seasons, rainy spring and dry autumn, cold winter, and hot summer. The annual average temperature is 18.4 degrees,

the average temperature of the hottest month is 30.6 degrees, the average temperature of the coldest month is 6.3 degrees, the annual maximum temperature is 43.1 degrees, the annual minimum temperature is -8.7 degrees; the annual average rainfall is 1341.5 mm, the annual maximum rainfall is 1835.2 mm.

2.2.2. Hydrogeology

The study area is located between the Songmu section on the west bank of the Xiangjiang River and the Chashan-Jinjialing section on the east bank of the Xiangjiang River, so data from the Xiangjiang River Watershed Hydrological Resources Survey was used. (in Table 1)

Table 1: Statistics on interannual variation of precipitation in Xiangjiang River waters Rainfall/mm

River Name	Age of data	Average annual rainfall	Maximum year		Minimum age	
			Precipitation	Year	Precipitation	Year
Xiangjiang River	2008-2018	1341.5	1835.2	2009	912	2013

According to the regional hydrogeological data and site investigation data, the type of groundwater in this sloped area is mainly bedrock fracture water, which is stored in the rock laminae and joints fractures, without stable groundwater level, often moving along the bedrock joints fracture surface, mainly recharged by surface water and atmospheric precipitation infiltration, with poor water quantity and small dynamic and magnitude changes. Strongly weathered and medium-weathered siltstone mudstones are weakly permeable, with a permeability of 4.65-8.86 Lu for the medium-weathered siltstone, which is a weakly permeable layer. No groundwater was encountered in any of the boreholes during the survey.

2.2.3. Topography

The geomorphological unit in the study area is a denuded remnant mound terrain. The topography is undulating, the overall topography is high in the south and low in the north, the highest elevation in the survey area is 103.27m, and the lowest elevation is 87.18m, the maximum difference in elevation after site leveling is 16.09m. The slope direction is 355 °, and the natural slope of the terrain is 25 °~35 °, the vegetation of the slope is not developed. Figure 2 shows the current situation after grading and excavation.

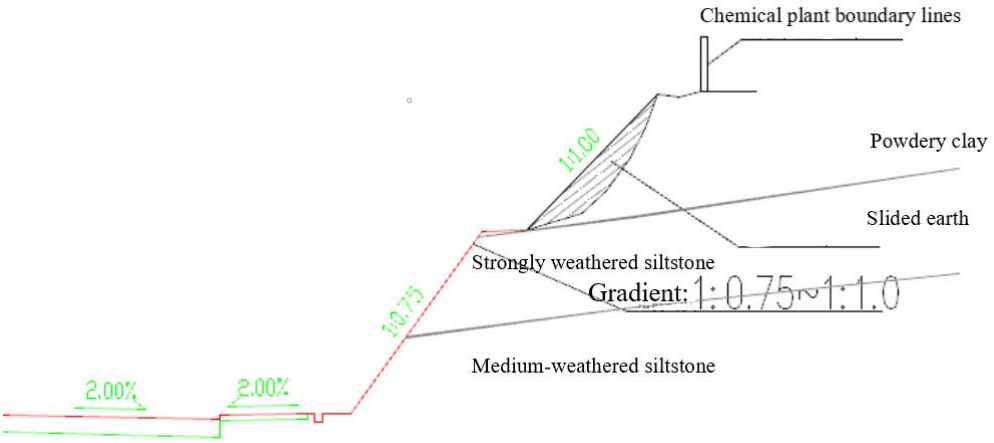

Figure 2: Schematic diagram of the landslide cross-section

2.2.4. Stratigraphic Lithology

Based on the results of the site survey, combined with the indoor geotechnical tests, the geotechnical layers within the slope support area are described from top to bottom as follows.

(1) Residual soils (chalky clay) (Q4el).

Maroon, slightly wet, plastic-hard plastic state, mainly composed of powder grains, powder grains to a lesser extent, locally containing weathered residual gravel, slightly shiny on the cut surface, no shaking reaction, medium-high dry strength, medium toughness. It is mainly distributed at the top of the slope, with an average thickness of 8.03m; the elevation of the surface is 73.04-94.74m.

(2) Strongly weathered siltstone mudstone (K).

Purple-red in colour, with much of the structure destroyed, weathering fissures well developed, the rock is fragmented, the cores are incomplete and fragmented, easily softened by water, and the rock is easily disintegrated by exposure. The rock integrity is extremely fragmented and the basic quality of the rock is grade V. The average thickness is 6.36m; The level elevation is 71.28-101.77m.

(3) Moderately weathered siltstone mudstone (K).

Purple-red, medium to thick-bedded, fractured, cores is short and long columnar, with black oxide film visible on the fracture surfaces and average structural surface bonding. The rock integrity is intact with a basic quality grade of IV. RQD > 80%.

The rock stratum in the survey area is generally a monoclinic structure, the production is stable, the local rock stratum is twisted, but the change is not significant, the rock stratum tendency is 345 °-355 °, tendency north, the dip angle is 20 °-30 °, the rock stratum tendency is the same as the slope direction, the slope angle is more than the rock stratum dip angle, if encounter special unfavorable factors, the possibility of sliding is greater, so take support measures. According to the geological mapping on site, the rock layer in the survey area is a medium-layered structure, with a layer thickness of about 0.1-0.5m and a general degree of structural surface bonding.

3. Numerical Simulation of Landslide Damage

3.1. Model Building

The calculation software uses Midas-GTS (SRM), which is based on the finite element strength discounting theory. The numerical simulation model was established based on the original slope profile. To meet the requirements of calculation accuracy and speed, the model was divided into 417 nodes and 335 grid cells, and the grid type was a plane strain cell. The boundary conditions of the model are: The left and right boundaries are horizontally constrained, the bottom edge is fully constrained; The top boundary and the slope surface are free boundaries. Considering the non-linear characteristics of the slope due to the deformation of the soil material, the elastic-plastic D-P principal model is used in this paper. Figure 3 shows the two-dimensional finite element model of the slope.

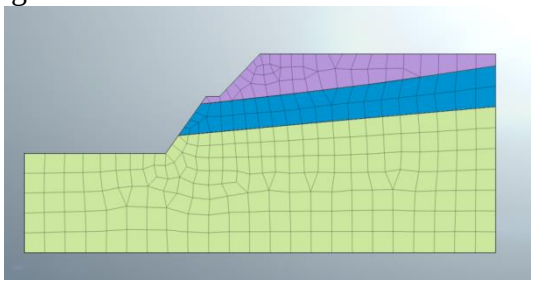

Figure 3: Two-dimensional finite element model of the slope

3.2. Calculation Parameters and Boundary Conditions

To analyze the influence of heavy rainfall on slope stability, this paper uses heavy rainfall conditions (2 ×10-3 m/h) according to the classification of rainfall by the Meteorological Bureau, with the initial state of the slope as the control group, and the rainfall ephemeris set at 4h, 8h, 12h, and 24h respectively. The left head height was 5.5m and the right head height was 9m.(in Table 2)

Table 2: Physical and mechanical parameters of the rock and soil

Geotechnical name	Modulus of compression Es (MPa)	Shear strength				Natural gravity γ (kN/m3)	Saturated gravity γ (kN/m3)
		Natural state		Saturated state			
		c (kPa)	φ (°)	c (kPa)	φ (°)		
Powdery clay	5.9	20.8	19.0	15.5	16.5	18.7	20.0
Strongly weathered siltstone mudstone	35.0*	50	30	35	28	22.0	23.0
Mid-weathering siltstone mudstone	/	200	40	160	38	25.5	26.0

4. Midas-GTS Calculation Results and Analysis

As can be seen from Table 3, the stability coefficient of the slope under complex working conditions tends to decrease as the duration increases, and the decrease is steep and then slow. At 3h, the stability coefficient is 1.694>1.3, which is stable; At 6h, the stability coefficient is 1.389≈1.3, which is stable; At 12h, the stability coefficient is 1.025≈1, which is less stable; At 24h, the stability coefficient is 0.947<1, which is unstable.

Table 3: Slope stability coefficients for different heavy rainfall epochs

Lasting	3h	6h	12h	24h
Stability factor	1.694	1.389	1.025	0.947

4.1. Influence of Different Heavy Rainfall Episodes on the Seepage Field of Slopes

The pore water pressure distribution of the slope under different heavy rainfall calendars is shown in Figure 4.

The pore water pressure distribution on the slope at different rainfall epochs is shown in Figure 5: As can be seen in Figures 4 and 5.

(1) It is shown in Figure 4 that throughout the rainfall process, the variation of the pore water pressure isopotential line no longer appears as a more regular horizontal line as the initial steady state seepage field, due to the different soil-water characteristic curves and saturation permeability coefficients of each geotechnical layer.

(2) Figure 5 shows that at 3h of rainfall, the pore water pressure near the slope node is still less than 0, and a large number of saturated zones have not yet appeared within the slope; After 6h of rainfall, the pore water pressure near the slope node is slightly greater than 0, and the rainfall further infiltrates and the saturated zones further increase.

(3) From Figures 4 and 5, it can be found that the slope has a saturated zone in the surface layer of the powdered clay at 3h and 6h of rainfall, but an unsaturated zone is silted up in the bottom layer of the powdered clay. As the rainfall duration increases, the water in the slope body continues to infiltrate and the unsaturated zone of the siltation of the bottom layer of the chalky clay gradually disappears. It is important to note that the unsaturated zone of slope siltation appears at the junction of the powdery clay and the strongly weathered mudstone, and the pore water pressure in the unsaturated

zone is negative, which means that the soil tends to swell and shear, indicating that the junction of the powdery clay and the strongly weathered mudstone of the slope is at risk of shear damage at 3h and 6h of rainfall history.

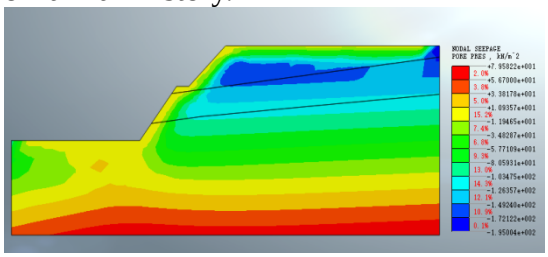

(a) 3h pore water pressure distribution

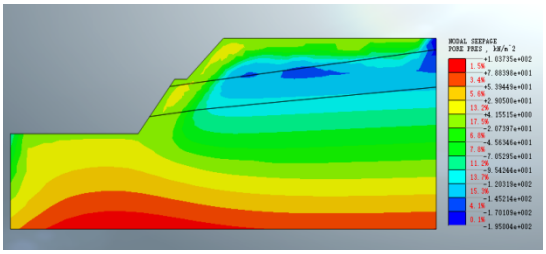

(b) 6h pore water pressure distribution

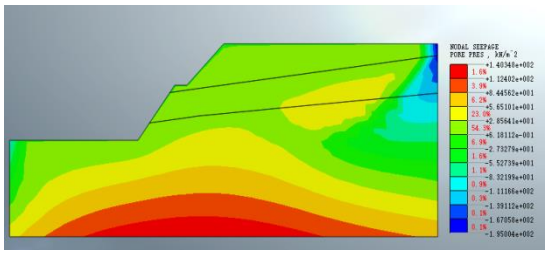

(c) 12h pore water pressure profile

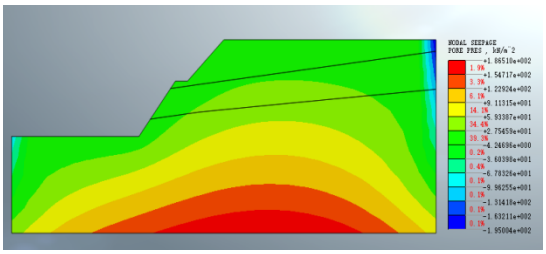

(d) 24h pore water pressure profile

Figure 4: Pore water pressure distribution on slopes for different heavy rainfall calendars

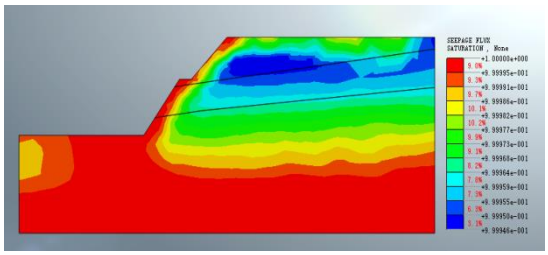

(a) 3h saturation distribution

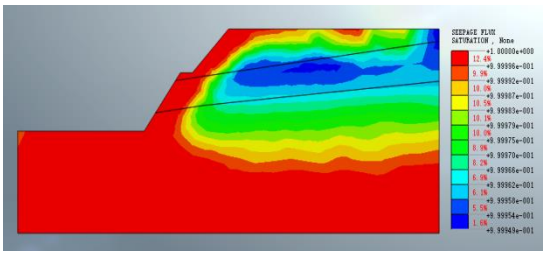

(b) 6h saturation distribution

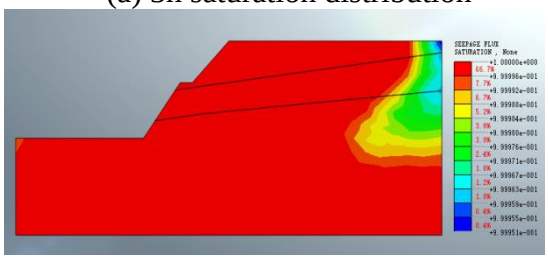

(c) 12h saturation profile

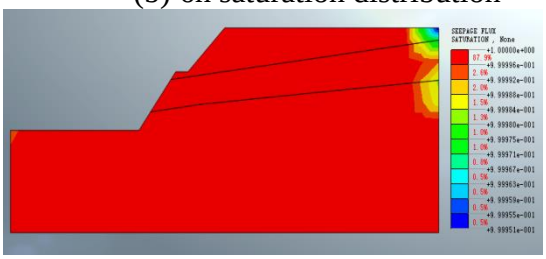

(d) 24h saturation profile

Figure 5: Distribution of slope saturation under different heavy rainfall epochs

4.2. Influence of Different Heavy Rainfall Epochs on the Slope Stress Field

The maximum shear strain distribution of the slope under different heavy rainfall calendars is shown in Figure 6.

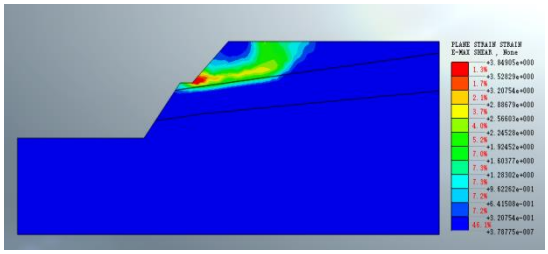

(a) 3h maximum shear strain cloud of the slope

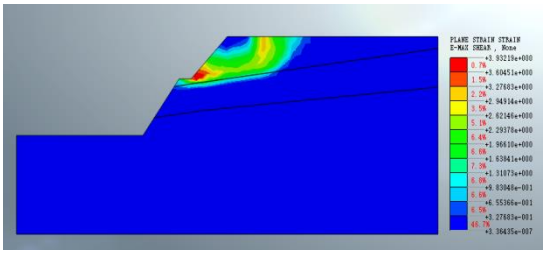

(b) 6h maximum shear strain cloud of the slope

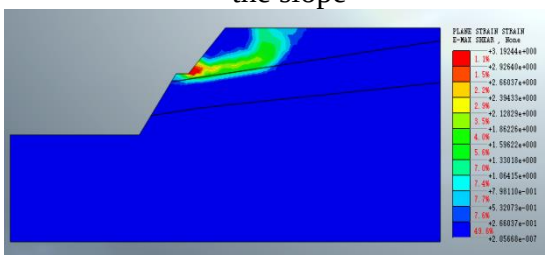

(c) 12h maximum shear strain cloud of the slope

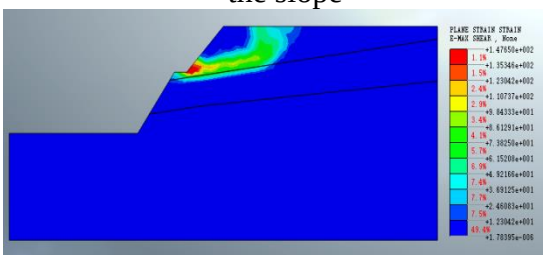

(d) 24h maximum shear strain cloud of the slope

Figure 6: Maximum shear strain clouds on slopes for different heavy rainfall epochs

As can be seen in Figure 6, the shear stresses at the toe of the primary slope, the toe of the secondary slope, and the platform are increasing over time. And the maximum shear strain in the slope is increasing with time. In particular, the maximum shear strain at 24h increased by 30 times compared to the maximum shear strain at 12h. This indicates that the geotechnical body of the slope is gradually saturated due to prolonged heavy rainfall, the overlying load is increasing, and the driving force of the landslide is increasing, coupled with further softening of the mudstone on the slip zone, the shear strength continues to decrease.

4.3. Influence of Different Heavy Rainfall Ephemeris on Slope Displacement

To further observe the precise variation of the slope displacement values, the 21 nodes (node 1 to node 21) of the drawn slope are arranged here, starting from the shoulder (node 1), from top to bottom, along the secondary slope, the platform, the primary slope up to the foot of the slope (node 21), as shown in Figure 7. The total displacements of the different nodes at different heavy rainfall epochs are shown in Figure 8.

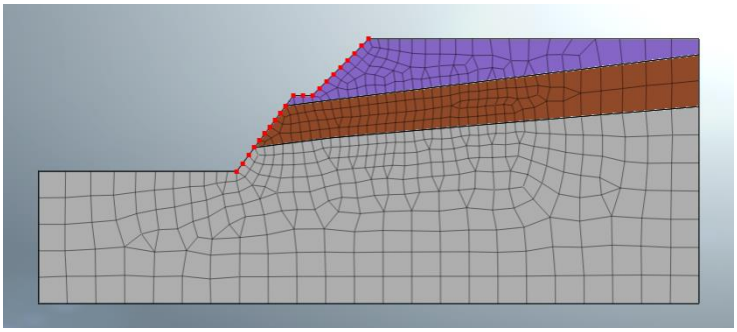

Figure 7: Extraction of nodes on the slope

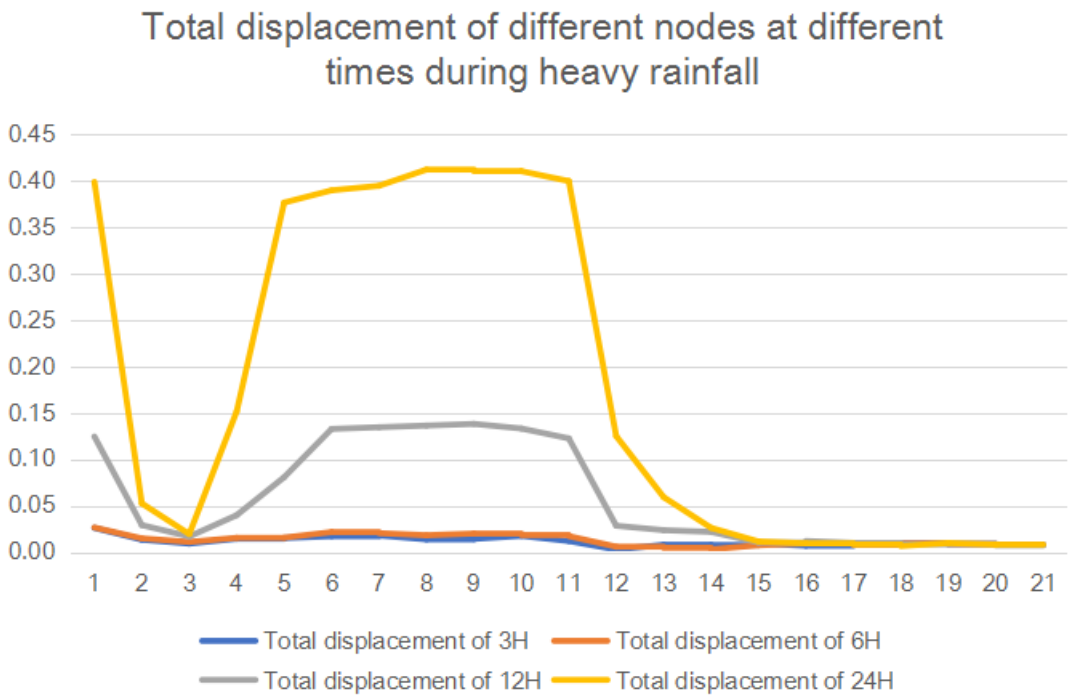

Figure 8: Total displacement of different nodes at different calendar times

As can be seen in Figure 8:

(1) The total displacement magnitude at different nodes under heavy rainfall conditions shows: large at the shoulder of the slope, large at the foot and platform of the secondary slope, larger at the waist of the secondary slope, and almost zero at the primary slope, similar to the "π" type.

(2) At 12h and 24h of rainfall, the slope is in an unstable and unstable state, and the displacement at different nodes of the slope surface varies very much at this time. The maximum nodal displacement at 24h of rainfall is nearly 300% higher than the maximum nodal displacement at 12h of rainfall.

5. Conclusion

In conjunction with the site survey, the factors influencing the landslide in an industrial park in Hunan include the relatively steep topography, the mud-rock binary structure combination, road construction, joint fracture development, and heavy precipitation.

The damage to the binary structure slope can be divided into four evolutionary processes: (1) Nurturing stage: After excavation and slope cutting, the strongly weathered layer and part of the medium weathered layer of mudstone are exposed to the air, and the rocks will be deformed after long-term weathering and water immersion, resulting in the reduction of their strength; (2) Cracking stage: As time passes, surface water continues to penetrate downward along the fissures and soil traps, resulting in the formation of multiple penetrating fissures inside the soil body formation of multiple penetrating fissures; (3) Creep phase: Frequent heavy rainfall causes the geotechnical body to gradually saturate, the overlying load continues to increase, the driving force of the landslide also continues to increase, the mudstone further softens, the geotechnical body shear strength decreases, and the slip zone gradually develops downward; (4) Sliding phase: Long-term precipitation causes the geotechnical body near the slip surface shear strength decreases, insufficient to support the upper load, the slip surface gradually develops through. (5) Sliding stage: Long-term precipitation causes the shear strength of the geotechnical body near the slip surface to decrease, which is insufficient to

support the upper load, and the slip surface gradually develops through. The absence of sliding at the toe of the primary slope and the collapse of the secondary slope from the top to the toe of the slope further confirm that the slope is a pushed landslide.

References

[1] Cao Songjie, Gao Jin, Wu Boqiang, Zhang Chao. Analysis of damage mechanism and prevention measures of landslide No.3 of Friendship Bridge in Zhangmu Town, Tibet. Roadbed Engineering, 2021 (05): 219-225. DOI:10.13379/j.issn.1003-8825.202008009.

[2] Wang Jiao, Hu Duiwen, He Kun, Cao Xichao. Numerical simulation of the deformation and damage mechanism of the landslide in Yangyuan County Glass Village based on Flac-3D. Geological Hazards and Environmental Protection, 2021, 32 (03): 11-17.

[3] Zhao Yonghui. Study on the characteristics of landslide development and damage mechanism of Yarlung Tsangpo River Highway. Highway, 2021, 66 (04): 6-10.

[4] Sun Y., Liu X. Stability analysis and design optimization of coal road graben slopes. People's Changjiang, 2020, 51 (S2):104-107. DOI: 10.16232/j.cnki.1001-4179.2020.S2.025.

[5] Li Zhiqiang, Xue Yiguo, Li Shucai, Zhang Lewen, Wang Dan, Li Bin, Zhang Wen, Ning Kai, Zhu Jianye. Deformation features and failure mechanism of deformation features and failure mechanism of steep rock slope under the mining activities and rainfall. Journal of Mountain Science, 2017, 14 (01): 31-45.

[6] Xu Jian, Wang Zhangquan, Ren Jianwei, Wang Songhe, Jin Long. Mechanism of slope failure in loess terrains during spring thawing. Mountain Science, 2018, 15 (04): 845-858.

[7] Hualin Cheng, Jiamin Zhou, Zhiyi Chen, Yu Huang. A Comparative Study of the Seismic Performances and Failure Mechanisms of Slopes Using Dynamic Centrifuge Modeling. Journal of Earth Science, 2021, 32 (05): 1166-1173.

[8] Sun F., Kong Jiming, Jia Chao, Xu Xingming. Deformation and damage mechanism of anti-slip piles on gravel soil landslides under earthquake action. Journal of the Changjiang Academy of Sciences, 2017, 34 (07): 77-81.

[9] Ai W., Wu H.G., Feng W.Q., Chen S.Y. Shaking table test research on deformation damage mechanism of multi-sliding surface landslide. Journal of Disaster Prevention and Mitigation Engineering, 2018, 38 (01): 65-71. DOI:10.13409/j.cnki.dome.2018.01.009.

[10] Zhou Qingfeng, Zhu Xingxian, Zhou Qigang. Study on the damage mechanism of the fractured bedrock landslide in Hushu Guangyang Mountain, Suzhou. Safety and Environmental Engineering, 2013, 20 (03): 27-31.

[11] Yin T.C., Yu L., Wang Y., Zhou H., Yao M., Huo Z.T. Study on the mechanism of landslide damage in near-horizontal strata under the action of fracture water. Safety and Environmental Engineering, 2020, 27 (05): 10-16.